Nickel hyperaccumulation is independent of the leaf economics spectrum, although it may be linked to plant water balance in an ultramafic plant community from Sabah (Malaysia)

Celestino Quintela-Sabarís, Michel-Pierre Faucon, Béatrice Gervais-Bergeron, Sukaibin Sumail, Antony van der Ent, Rimi Repin, John Sugau, Reuben Nilus, Thomas Rigaudier, Guillaume Echevarria, et al.

Nickel hyperaccumulation is independent of the leaf economics spectrum, although it may be linked to plant water balance in an ultramafic plant community from Sabah (Malaysia)

Celestino Quintela-Sabarís[1,2]*, Michel-Pierre Faucon[3], Béatrice Gervais-Bergeron[4,5], Sukaibin Sumail[6], Antony van der Ent[2,7], Rimi Repin[6], John Sugau[8], Reuben Nilus[8], Thomas Rigaudier[9], Guillaume Echevarria[2], Sophie Leguedois[2]

[1] Universidade de Vigo, Grupo de Agrobioloxía Ambiental: Calidade, Solos e Plantas (BEV1), 36310 Vigo, Spain

[2] Université de Lorraine, INRAE, Laboratoire Sols et Environnement, 54000 Nancy, France

[3]AGHYLE, Agroécologie, Hydrogéochimie, Milieux et Ressources (UP.2018.C101), Institut Polytechnique UniLaSalle, Beauvais, France.

[4]Faculté de l'Aménagement, École d'urbanisme et d'architecture de paysage, Université de Montréal, QC, Canada

[5]Institut de recherche en biologie végétale, Université de Montréal, QC, Canada

[6]Sabah Parks, Kota Kinabalu, Sabah, Malaysia

[7]Centre for Mined Land Rehabilitation, Sustainable Minerals Institute, The University of Queensland, Queensland, Australia

[8]Forest Research Centre, Sabah Forestry Department, Sandakan, Sabah, Malaysia

[9]Univ Lorraine and CNRS, CRPG, UMR 7358, 54501 Vandoeuvre-lès-Nancy, France

*** Correspondence:**
Celestino Quintela-Sabarís
celestino.quintela@uvigo.gal

Authors' ORCID;

Celestino Quintela-Sabarís: 0000-0002-1795-2011

Michel-Pierre Faucon: 0000-0001-5448-7932

Béatrice Gervais-Bergeron: 0000-0002-0489-0122

Antony van der Ent: 0000-0003-0922-5065

Reuben Nilus: 0000-0001-7300-1360

Thomas Rigaudier: 0000-0003-4947-3784

Guillaume Echevarria: 0000-0003-2124-1447

Sophie Leguédois: 0000-0001-9210-1340

Abstract

Background and aims

Nickel (Ni) hyperaccumulators are a group of plants able to store elevated amounts of this element in their leaves. Some studies indicate that hyperaccumulation may be associated with traits favouring fast resource capture or with traits favouring nutrient and water conservation, but there is no evidence for the role of nickel hyperaccumulation in the leaf economics spectrum. Our study aims to assess the differences in the leaf economics spectrum between Ni hyperaccumulators and non-hyperaccumulators.

Methods

We have conducted a field study involving five hyperaccumulators and ten non-hyperaccumulators growing on the same ultramafic community in Sabah (Malaysia). We measured two structural and seven chemical leaf traits and computed a Principal Component Analysis, which was complemented by a test of the phylogenetic signal of each trait and linear mixed models to assess the influence of each leaf trait on nickel accumulation.

Results

Our analyses inferred three principal components that reflected the main environmental constraints that shape the resource acquisition strategies of the studied ultramafic plant community: leaf economics spectrum, hyperaccumulation and water-use efficiency, and calcium to magnesium balance. Moreover, the linear mixed models indicated that carbon isotope discrimination and potassium concentrations had a significant effect on Ni accumulation, suggesting that nickel might replace partially potassium in its role in plant water balance.

Conclusion

Overall, the data suggest that in the community studied, Ni hyperaccumulation is independent of the leaf economics spectrum and related to plant water economy. More studies with other hyperaccumulator plants are needed to confirm these findings.

Keywords: Borneo, functional ecology, scrubland, tropics, ultramafic areas

Introduction

Hyperaccumulators are plant species able to uptake from soil, transport, and store in their aerial biomass extremely high concentrations of trace elements over a defined hyperaccumulation threshold, without suffering phytotoxic effects (Rascio and Navari-Izzo 2011; Reeves et al. 2018; van der Ent et al. 2013). Hyperaccumulation thresholds are metal(loid) levels two to three orders of magnitude higher than those in 'normal' plants and one order of magnitude higher than non-hyperaccumulators growing on metal-rich soils (van der Ent et al. 2013). Thus, the threshold concentration depends on the metal considered and varies from 100 μg g^{-1} (0.01% in dry weight-DW) for cadmium (Cd) to 10,000 μg g^{-1} (1% DW) for manganese (Mn).

To date, more than 700 metal(loid) hyperaccumulator plant species have been described (Krämer 2010; van der Ent et al. 2013; Rascio and Navari-Izzo 2011; Reeves et al. 2018), of which three-quarters are nickel (Ni) hyperaccumulators; that is, plants which Ni concentration in their leaves is higher than 1000 μg g^{-1}, or 0.1% biomass DW. The high percentage of Ni hyperaccumulators has been explained by the large number of Ni-enriched soils derived from ultramafic rocks worldwide (Baker et al. 2000; Brooks 1987). Nickel hyperaccumulators are mainly found in Eudicots, with some orders (Buxales, Oxalidales, Mapighiales, and Brassicales) having a high percentage of hyperaccumulating species (Jaffré et al. 2013).

Several theories have been proposed to explain the role of metal hyperaccumulation and its evolutionary significance: metal tolerance/disposal (i.e. hyperaccumulation is a tolerance mechanism that allows sequestration of metals in tissues and its disposal from plant body by the shedding of those high metal tissues), inadvertent uptake (i.e. hyperaccumulation is an inadvertent consequence of other processes such as efficient nutrient uptake), drought resistance (i.e. hyperaccumulated metal can reduce cuticular transpiration or it has a role in osmotic adjustment), interference with neighboring plants and defence against herbivores and/or pathogens (Boyd 2004; Kazakou et al. 2008; Pollard et al. 2014; Rascio and Navari-Izzo 2011). To date, the role of metal hyperaccumulation in interference -'elemental allelopathy'- (Adamidis et al. 2016; El Mehdawi and Pilon-Smits 2012) and defence against natural enemies (Boyd 2007; El Mehdawi and Pilon-Smits 2012; Fones et al. 2013) have obtained direct and indirect support in different hyperaccumulators. In contrast, the influence of hyperaccumulation on the response to drought has been found in only one species (Bhatia et al. 2005), and indications of inadvertent uptake have been found in two hyperaccumulators from the Brassicaceae family (Meindl et al. 2021).

Plant functional traits are morpho-physio-phenological traits which affect fitness indirectly via their effects on growth, reproduction, and survival (Garnier et al. 2004; Garnier and Navas 2013). For example, the specific leaf area (SLA) is positively related to growth rate (Cornelissen et al. 2003), i.e. high SLA equates to a larger light-intercepting leaf area for a given investment in leaf mass,

which allows faster growth. Another example is carbon isotope discrimination (Δ), a parameter determined by the Rubisco activity and the diffusion of CO_2 from the atmosphere into the leaf, which is in turn influenced by stomatal conductance (Lambers et al. 2008). Thus, Δ is used as a proxy of water use efficiency in C3 plants (Farquhar et al. 1989). The observation of a strong correlation among different leaf functional traits led to the description of a global "leaf economics spectrum" (Wright et al. 2004). This spectrum ranges from conservative (i.e. species with long-lived leaves with low specific leaf area, low leaf nitrogen -N- and phosphorus -P- concentrations, and low photosynthetic capacity) to acquisitive strategies (i.e. species with short-lived leaves with high specific leaf area, high N and P and high photosynthetic capacity). Further studies have extended the concept of economic spectrum to other plant organs (roots, stems, diaspores) and related it to stress factors such as drought (Diaz et al. 2016; Reich 2014). Thus, the key traits involved in carbon, nutrient and water economics vary in coordinated ways both within and among plant individuals, and acquisitive (i.e. fast) strategies are favoured in resource-rich environments, whereas the more conservative (i.e. slow) strategy is best suited to resource-poor sites (Reich 2014). Metal hyperaccumulation can be also considered a functional trait (Lange et al. 2017), with known effects in defence and competition (see above). However, the relationship between hyperaccumulation and leaf economics spectrum has not yet been explored. Different studies on the physiology of Zn, Cd, and Ni hyperaccumulation indicate that this trait is the result of the exaggeration of basic mechanisms involved in metal homeostasis, such as the overexpression of IREG/Ferroportin transporter (normally involved in the efflux of Fe to the vacuole) in Ni hyperaccumulators or the gene duplication and overexpression of the *HMA4* gene, which increases xylem Zn loading and induces the overexpression of several ZIP genes, normally induced by Zn-deficiency, in *Arabidopsis halleri* (L.) O'Kane & Al-Shehbaz and possibly in other Zn hyperaccumulators (García de la Torre et al. 2021; Merlot et al. 2018). Moreover, it has been observed that manganese (Mn) accumulation is correlated to efficient mechanisms of soil P mobilisation and absorption (Lambers et al. 2015), as happens in the Mn-hyperaccumulator *Phytolacca americana* L. (DeGroote et al. 2018). Overall, these findings suggest a possible relation between metal hyperaccumulation and efficient nutrient mobilisation or uptake (i.e. inadvertent uptake). If this relation exists, we could expect that in nutrient-poor ultramafic areas non-hyperaccumulators would have a conservative (i.e. "slow") strategy whereas hyperaccumulators would show higher nutrient concentrations and a more acquisitive (i.e. "faster") strategy. To explore the links between Ni-hyperaccumulation and leaf economics spectrum, we have quantified and compared two structural and seven chemical leaf traits in fifteen plant species (five Ni hyperaccumulators and ten non-hyperaccumulators) from the same ultramafic plant community (Bukit Lompoyou, Sabah, Malaysian Borneo). The presence of several hyperaccumulators in the

same area allowed us to reduce the effect of environmental heterogeneity on our comparisons between groups of species and we also applied a correction to eliminate possible phylogenetic bias.

Material and methods

Sampling site

Sabah (N of Borneo, Malaysia) hosts extensive ultramafic areas (3500 km^2, around 5% of its land surface, Proctor et al. 1988) where about 30 Ni hyperaccumulators have been described (van der Ent et al. 2019, 2015a). This study has been carried out near the summit area of an ultramafic hill (Bukit Lompoyou) bordering Kinabalu Park (Sabah, Malaysia) (coordinates N 06°06’53’’ E 116°44’55’’, around 700 m asl). Bukit Lompoyou has been burnt at least once as a result of an uncontrolled forest fire in the late 2000s. Prior to burning, the site had already been heavily disturbed by logging. Currently, the site has a short and open scrub community (dominated by shrubs 1–3 m tall) with the presence of several Ni hyperaccumulators. In fact, this area is the type locality for the hyperaccumulator *Actephila alanbakeri* Welzen & Ent (van der Ent et al. 2015b). The studied area has a S-SW aspect and steep slopes (around 30%). Soils (Hypermagnesian Cambisols) are shallow and quite heavily eroded, with frequent exposed bedrock and saprolite (van der Ent et al. 2017). The climate is tropical with a mean annual temperature of 23 °C with low variation (< 3 °C) throughout the year. The annual rainfall around Kinabalu Park is evenly distributed throughout the year and is approximately 2500 mm, although two less humid periods in February and August are typical (Aiba and Kitayama 1999; Kitayama et al. 1998 and Malaysian meteorological department). In spite of this benign climate, shallow soils and steep slopes make local conditions xeric.

Figure 1: Studied site. **A,** regional map. **B**, local map. Dark grey areas mark Malaysia in the regional map, and natural Parks of Sabah in the local map. Red circle marks the area of study (Lompoyou Hill) in the North of Borneo, East border of Kinabalu Park. **C**, general overview of studied area (July 2016). Invasive *Chromolaena odorata* is present in high density in the foreground (oil-palm estate on ultramafic soil) whereas the undisturbed primary forests of Kinabalu Park can be seen in the background.

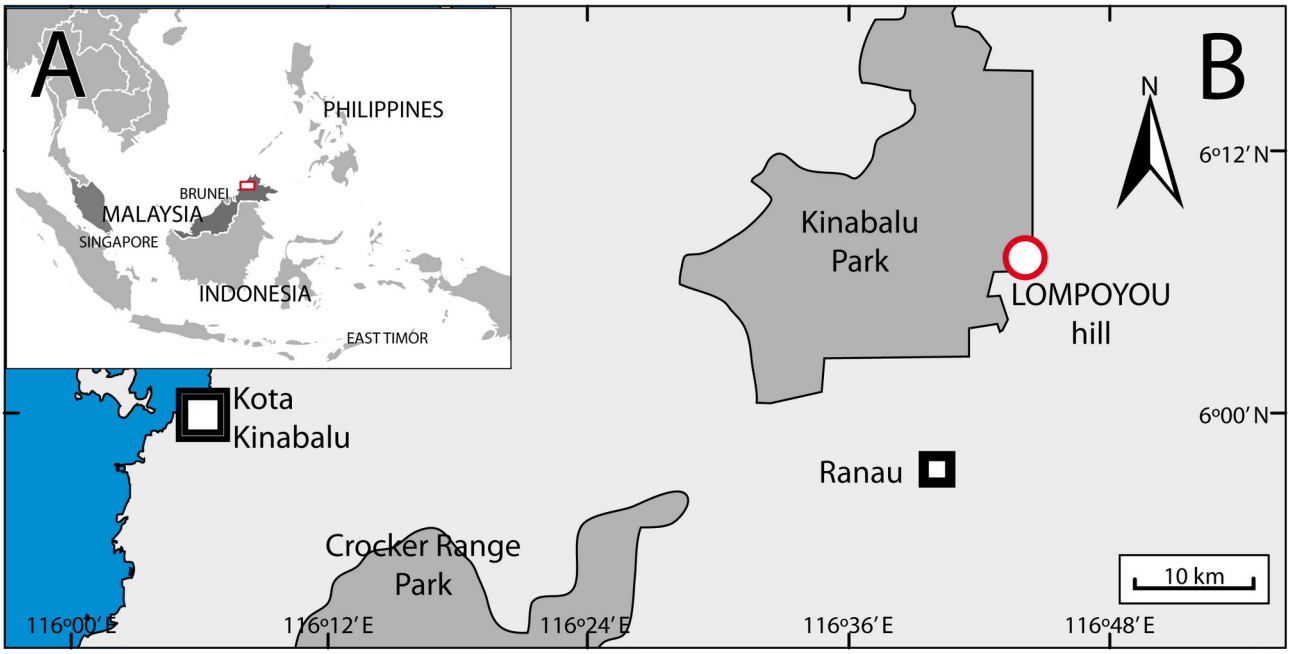

Sample collection

A linear transect was established along the Kinabalu Park boundary near the summit area of Lompoyou Hill (Bukit Lompoyou) (Figure 1). Ten non-hyperaccumulator (NH) species were selected along that transect, plus five known Ni hyperaccumulators (H, van der Ent et al. 2015a) growing in the same area, giving a total of 15 sampled species that are dominant in this site (Table 1). All the 15 species are Dicot shrubs/small trees with C_3 photosynthesis (measured $\delta^{13}C$ values between -33 and -25‰, see results). Fourteen species are native to Borneo, whereas the NH *Chromolaena odorata* (L.) R.M.King & H.Rob. (Asteraceae), commonly present in degraded areas on different kind of substrates in Sabah, is a Neotropical shrub that currently is widespread in tropical Asia and Africa (Van Gils et al. 2004). For each species, six plants fully exposed to sunlight were selected and branches with leaves were collected, totalling 90 sampled individuals. Upon sampling, branches were kept in closed plastic bags and transported to Sabah Parks Herbarium (SNP), where they were processed the same day of sampling. A soil sample (fresh weight around 300 g) was collected from the A horizon beneath the canopy of each sampled plant. Soil samples from each species were mixed together to obtain a composite soil sample per species, totalling 15 composite soil samples.

Table 1: List of sampled species. In several cases, identification was possible only to genus level. For each species, plant family (following APG IV) is included. Type refers to hyperaccumulator (H) or non-hyperaccumulator (NH) status.

CODE	Species/Genus	Family (APG IV)	Type
ACAL	*Actephila alanbakeri* Welzen & Ent	Phyllanthaceae	H
ALSP	*Alstonia* sp. R.Br.	Apocynaceae	NH
ARSP	*Ardisia* sp. Sw.	Primulaceae	NH
CHOD	*Chromolaena odorata* (L.) R.M.King & H.Rob.	Asteraceae	NH
CRSP	*Croton* sp. L.	Euphorbiaceae	NH
DEFR	*Decaspermum fruticosum* J.R.Forst. & G.Forst.	Myrtaceae	NH
EMRU	*Emblica rufuschaneyi* (Welzen, R.W.Bouman & Ent) R.W.Bouman	Phyllanthaceae	H
MAKI	*Macaranga kinabaluensis* Airy Shaw	Euphorbiaceae	NH
MESP	*Melastoma* sp. L.	Melastomataceae	NH
PTSP	*Pterospermum* sp. Schreb.	Malvaceae	NH
RILI	*Rinorea linearifolia* Latiff	Violaceae	H
SASP	*Sapium* sp. Jacq.	Euphorbiaceae	NH
TISP	*Timonius* sp. Rumph. ex DC.	Rubiaceae	NH
WAPI	*Walsura pinnata* Hassk.	Meliaceae	H
XYLU	*Xylosma luzonensis* Clos	Salicaceae	H

Analysis of soil and plant samples

Soils were dried at 40º C until constant weight and sieved (< 2 mm). Water retention data were determined on a pressure plate apparatus for two water potentials (-10 kPa & -15800 kPa) according to the methods described by Bruand et al. (1996). The available water storage (AWS), i.e. water disposable for plant growth , was calculated using the following equation: AWS=(Wfc−Wwp), where AWS represents the available water storage (g 100 g^{-1}), Wfc is the water content at field capacity (g 100 g^{-1}) (water potential: - 10 hPa), Wwp is the water content at permanent wilting point (g 100 g^{-1}) (water potential: - 15800 hPa). Soil pH was measured in H_2O, after 60 min shaking, using a 1:5 (v/v) ratio. Cation Exchange Capacity (CEC) was determined colorimetrically after treatment of the soil with a solution of cobalt hexamine trichloride 0.05 N, following the standard method AFNOR NF X31-130 (AFNOR, 1999). Exchangeable concentrations of Ca^{+2}, K^{+}, Mg^{+2} and Ni^{+2} in the soil were determined on the filtered soil-cobalt hexamine extracts by ICP-AES (Liberty II, Varian). For most of the soil samples concentrations of exchangeable Na^{+} were below the limit of quantification, so this cation was not evaluated. Soil available phosphorus (Olsen-P) was extracted with a solution of $NaHCO_3$ and quantified by reaction with ascorbic acid, following the standard method AFNOR NF ISO 11263 (AFNOR, 1995). Soil nickel availability was evaluated after extraction with DTPA-TEA (0.005 M DTPA with 0.01 M $CaCl_2$ and 0.1 M triethanolamine (TEA) at pH 7.3; ratio 1:2 soil:extracting solution w/v, 2h shaking) (Lindsay and Norvell 1978). Soil subsamples were ground in a ceramic mortar and 0.5 g of dry ground soil was digested in 2 mL of concentrated HNO_3 and 6 mL of concentrated (37%) HCl on a hot plate at 105°C. The final solutions were filtered (0.45 µm DigiFILTER, SCP science, Canada) and brought to volume (50 mL) with deionised water. Pseudo-total soil concentrations of Al, Ca, Co, Cu, Cr, Fe, K, Mg, Mn, Ni, P, S and Zn were determined by analysis of the digests with ICP-AES (Liberty II, Varian). Total soil C and N concentrations were estimated by combustion of dry ground soil subsamples in a CHNS analyser (Vario Micro Cube, Elementar, Germany). All soil analyses were performed in triplicate for each composite soil sample.

The bags containing the branches were opened at the laboratory on the same day they were sampled. There, three healthy fully expanded leaves were collected per plant and kept overnight between water damp papers in sealed bags at 5ºC in the dark to obtain a standard turgor (Wilson et al. 1999). Then, each leaf, including the petiole, was blotted with tissue paper to remove surface water andweighed to obtain leaf fresh weight (FW). Then, the leaf was placed below a layer of glassand photographed with a digital camera. The camera was placed on a fixed support to guarantee its orthogonal position with respect to the leaves. In some cases (e.g. curved leaf midrib), the leaf was cut in several fragments to ensure the correct estimation of leaf area. All leaf photographs included a ruler to allow the estimation of leaf area. Leaf area was obtained from the

digital photographs using ImageJ software (Schneider et al. 2012). After weighing and photographing, each leaf was cleaned with tap water, rinsed with deionised water and put in a paper envelope. The leaves were kept in an oven (60ºC) until constant weight and leaf dry weight (DW) was obtained. The specific leaf area (SLA) was calculated as the ratio between leaf area and dry leaf mass, including petiole. Leaf dry matter content (LDMC) was computed as the ratio of the leaf dry weight divided by its fresh weight. Then, the three samples from each plant were put together and finely ground using a ball mill. Subsamples (0.5 g) of dry and ground tissues were digested at 95°C in 2.5 mL of concentrated HNO_3 and 5 mL of H_2O_2 (30%). The final solutions were filtered (0.45 µm DigiFILTER) and diluted up to 25 mL with deionised water. The foliar concentrations of the elements Ca, K, Mg, Ni, and P were measured by ICP-AES (Liberty II, Varian). Leaf C and N concentrations and C isotope signatures ($\delta^{13}C$) were quantified in dry ground by combustion in a Thermo Scientific EA IsoLink IRMS System at CRPG laboratory (Nancy, France). Carbon isotope discrimination (Δ) was computed using the formula: $\Delta = (\delta_a - \delta_p) * (1 + \delta_p)^{-1}$ (Farquhar et al. 1989); where δ_a is the isotopic signature of air (approximately – 8 ‰) and δ_p is the measured isotopic signature of the plant.

Statistical analyses

To assess soil variability underneath hyperaccumulators and non-hyperaccumulators, the differences between the collected soils were explored by one-way ANOVAs with *Type* (hyperaccumulator and non-hyperaccumulators) as a fixed factor. The leaf traits (SLA, LDMC, foliar concentrations of Ca, K, Mg, N, Ni, and P, and Δ) were analysed by Principal Components Analysis (PCA). The PCA was based on a correlation matrix of the $\log_{10}$ transformed variables. This approach is equivalent to using standardized data and is considered appropriate for data with different measurement scales (Diaz et al., 2016). We kept the Principal Components (PCs) with eigenvalues higher than 1. We analysed the plants' scores on those PCs by nested ANOVAs (nANOVAs) with *Type* (hyperaccumulator or non-hyperaccumulator) as a fixed factor and *Species within Type* as a random factor. One-way ANOVAs, PCA and nANOVAs were obtained with SPSS (v. 15.0, SPSS Inc., Chicago, IL, USA).

Although Ni hyperaccumulators are scattered along the Eudicot clade there are some phylogenetic patterns (e.g. two thirds belong to the COM clade (Celastrales, Oxalidales and Malpighiales) (Jaffré et al. 2013) that need to be considered in the analyses. Therefore, we constructed a phylogeny of the 15 species included in our study using the function *phylo.maker()* from the R package *V.PhyloMaker* (version 0.1.0; Jin and Qian 2019) based on a mega-tree (GBOTB.extended.tre, provided in the package *V.PhyloMaker*), containing 10,587 genera and 74,533 vascular plant species. The *phylo.maker()* function in *V.PhyloMaker* makes phylogenetic hypotheses in three

scenarios (Jin and Qian 2019), and we chose scenario 3 (the tip for a new genus is bound to the 1/2 of the family branch and the new tip of an existing genus is bound to the basal node of a given genus), which is robust enough to be used in studies of community ecology (Qian and Jin 2016). Then, we used this phylogeny to evaluate the phylogenetic signal (Pagel's λ) of every trait, testing if the signal is significantly different than 0 with the *phylosig*() function (*phytools* package, v. 1.9-16; Revell 2012) in R (version 3.6.3; R Core Team 2020).

The impact of individual traits on Ni accumulation in leaves was analysed using linear mixed effect models (function *lmer()*, Package *lmerTest*, v. 3.1-3; Kuznetsova et al. 2020). All variables were log-transformed and set as fixed factors, with Ni as the response variable and the species as random factors. To test whether phylogenetic structure had a significant impact on Ni and trait relationships, species' families and clades were further added to the model as clustered random factors. An ANOVA determined whether the phylogenetic structure significantly improves the fit of the data, based on the model residual sum of squares (function *anova*). Subsequently, a model selection, based on AIC criteria (function *step()*, Package *AICcmodavg*, v. 2.3-1; Mazerolle 2020), determined the best combination of traits to explain Ni accumulation. A non-significant difference ($P > 0.05$) between models indicates that the simpler model should be kept. Similarly, a model selection process was further repeated on the hyperaccumulator and non-hyperaccumulator groups, since Ni leaf accumulation is distinctly distributed into two bell shapes (Fig. S1), suggesting a potentially distinct model within each group.

All analyses were performed in R (version 3.6.3; R Core Team 2020) using the R Studio environment (version 2023.090+463; Posit team, 2023).

Results

Soils

Sampled soils were slightly acidic (pH = 6.72) and had typical ultramafic conditions, such as very low concentrations of essential nutrients, high iron concentration and high concentration of trace elements Ni, Cr and Co. Thus, the average pseudo-total concentrations of P and K were 211 and 254 mg kg^{-1}, respectively; the average pseudo-total Fe concentration was around 117 g kg^{-1}; and the average pseudo-total concentrations of Ni, Cr and Co were 2561, 4534 and 490 mg kg^{-1}, respectively (table S1). Moreover, exchangeable and DTPA-extractable Ni concentrations were relatively high (0.11 $cmol_c$ kg^{-1} and 271 mg kg^{-1}, respectively). Although the pseudo-total Mg concentration was much higher than the pseudo-total Ca concentration (Ca:Mg ratio of 0.26), the molar ratio of exchangeable Ca and Mg was 1.71 (i.e. almost two mols of Ca per mol of Mg), a value that is not typical of ultramafic soils. None of the soil parameters was significantly different

between samples collected beneath hyperaccumulators and non-hyperaccumulators, indicating that the different amounts of Ni or other elements measured in plants are due to different plant strategies rather than soil conditions.

Phylogenetic clustering

The dendrogram showed some phylogenetic clustering of the hyperaccumulators. Four of them (*A. alanbakeri*, *E. rufuschaneyi*, *R. linearifolia* and *X. luzonensis*) were grouped in a single clade, sister to the Euphorbiaceae species *Croton* sp., *M. kinabaluensis*, and *Sapium* sp. (Figure 2), both of them within the Order Malpighiales. The other hyperaccumulator (*W. pinnata*, Order Sapindales) was sister to the non-hyperaccumulator *Pterospermum* sp. (Order Malvales). Still, no significant phylogenetic signal (Pagel's λ) was detected in the Ni accumulation trait (λ = 0.74, P = 0.21). Neither were signals detected for nutrient accumulation (N, P, K, Ca, or Mg) or Δ (Table S2). However, specific leaf area (λ = 1.64, P = 0.02) had a significant phylogenetic signal and LDMC a tendency (λ = 1.23, P = 0.06).

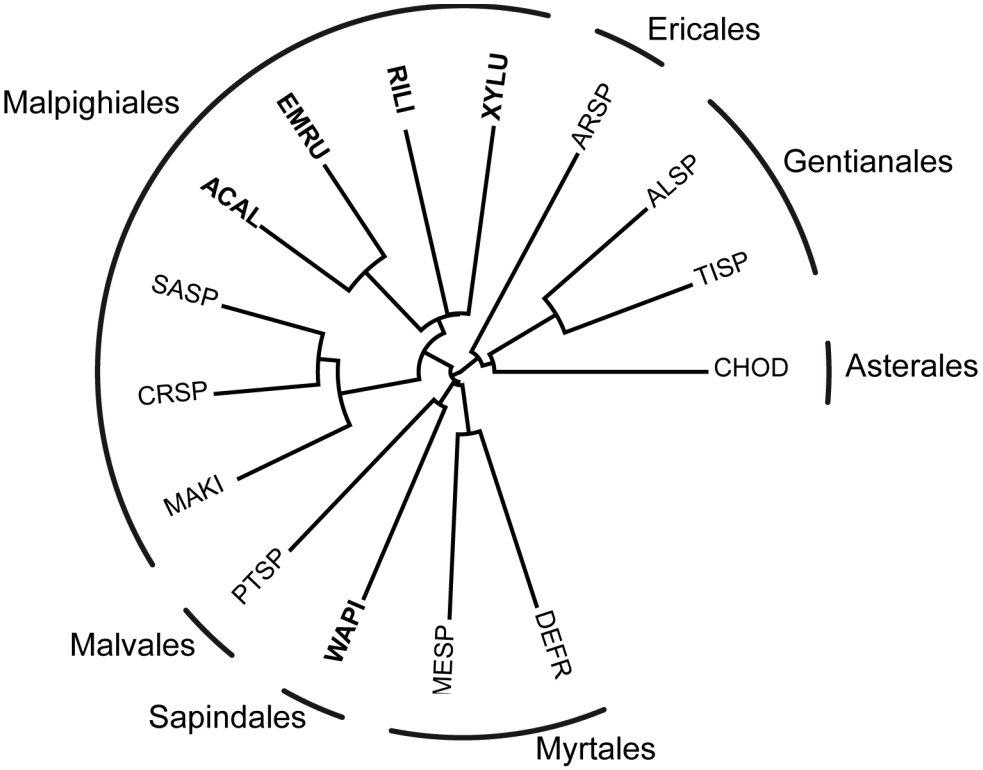

Figure 2: Radial dendrogram showing the phylogenetic relationships between the 15 plant species included in this study and to which Order they belong. The presented relationships were used to assess the presence of phylogenetic signal on the leaf traits. Nickel hyperaccumulators are marked in **bold** type. For plant codes, see table 1.

Plant traits

Ni foliar concentrations in non-hyperaccumulators were around 37.5 µg g^{-1}, with the exception of *Sasium* sp., which had Ni concentrations around 200 µg g^{-1} (Table 2). The average Ni concentration in hyperaccumulators was 9500 µg g^{-1}, with values ranging from 1000 µg g^{-1} in *Walsura pinnata* to 40,000 µg g^{-1} in one individual of *Emblica (Phyllanthus) rufuschaneyi.* This last species was the strongest hyperaccumulator in our dataset, with average foliar Ni concentrations around 24,000 µg g^{-1} (Table 2).

With the exception of Ni, the other foliar traits had overlapping ranges in hyperaccumulators and non-hyperaccumulators (Table 2). The average values of LDMC and SLA were around 400 mg g^{-1} and 10 mm^2mg^{-1}, respectively. Carbon isotope discrimination ranged from 18.4 ‰ to around 25 ‰ both in hyperaccumulator and non-hyperaccumulator species (Table 2). The mean foliar concentrations of Ca, N, and K were around or higher than 1 wt% of dry leaf biomass. The highest foliar Ca concentrations were in the non-hyperaccumulator *Melastoma* sp. (average 34 mg g^{-1}), whereas the highest foliar Mg was in the non-hyperaccumulator *Chromolaena odorata* (average above 10 mg g^{-1}) (Table 2). The average foliar concentration of K in two hyperaccumulators (*Actephila alanbakeri* and *Walsura pinnata*) was greater than 20 mg g^{-1} (Table 2).

Table 2: Average attributes of nine leaf traits in 15 plant species (five Ni hyperaccumulators -H-, and ten Non-hyperaccumulators -NH-) from the ultramafic area of Bukit Lompoyou. For plant codes, see table 1. *LDMC*, leaf dry matter content; *SLA*, specific leaf area; *Δ*, carbon isotope discrimination; *N*, *P*, *K*, *Ca*, *Mg* and *Ni* are the foliar concentrations of each of those elements.

Species	**Type**	**LDMC** (mg g^{-1})	**SLA** (mm^2 mg^{-1})	**Δ** (‰)	**N** (mg g^{-1})	**P** (mg g^{-1})	**K** (mg g^{-1})	**Ca** (mg g^{-1})	**Mg** (mg g^{-1})	**Ni** (µg g^{-1})
ACAL	H	302	9.24	20.56	36.7	0.86	25.4	17.2	2.3	8,178
ALSP	NH	265	12.75	21.59	25.5	0.79	17.5	15.4	4.9	17
ARSP	NH	396	8.33	24.13	17.0	0.54	10.0	25.9	1.3	11
CHOD	NH	254	22.39	25.13	32.0	1.01	11.4	14.6	10.2	36
CRSP	NH	439	8.4	21.76	20.5	0.65	12.6	11.6	4.3	5
DEFR	NH	446	7.48	24.48	14.2	0.44	6.3	11.3	2.7	21
EMRU	H	404	11.58	23.13	22.0	0.85	12.0	9.3	2.4	24,000
MAKI	NH	451	7.97	21.25	11.8	0.36	3.9	6.3	1.3	31
MESP	NH	446	7.34	22.59	14.0	0.39	4.5	34.3	2.2	17
PTSP	NH	500	7.26	19.43	16.0	0.54	7.9	14.2	3.1	14
RILI	H	420	6.57	19.92	17.3	0.69	12.1	14.3	3.0	7,850
SASP	NH	448	9.46	20.84	18.2	0.61	3.7	4.8	6.8	206
TISP	NH	338	17.17	23.83	20.0	0.50	13.6	14.6	3.8	18
WAPI	H	440	7.05	21.6	19.7	0.69	20.6	11.3	1.8	1,897
XYLU	H	476	10.71	24.14	20.3	0.57	13.9	22.7	2.6	5,510
Mean ± SD for H		408 ± 65	9.0 ± 2.2	21.9 ± 1.8	23.2 ± 7.7	0.73 ± 0.12	16.8 ± 6.0	14.9 ± 5.3	2.4 ± 0.4	9500 ± 8520

Mean ± SD for NH	398 ± 84	10.9 ± 5.1	22.5 ± 1.8	19.0 ± 6.0	0.58 ± 0.20	9.2 ± 4.7	15.3 ± 8.8	4.1 ± 2.7	37.5 ± 59.9
Mean value in TRY database[1]	213	16.6	-	17.4	1.23	8.4	9.1	2.6	-
Mean value for evergreen angiosperms[2]	-	-	-	17.3	1.3	8.8	11.6	3.7	-

[1] Kattge et al. (2011)
[2] Vergutz et al. (2012)

The PCA inferred three PCs explaining 76% of total variation in leaf dataset (Table 3). The first PC (PC1, 41% of variation) had positive correlations with specific leaf area and foliar concentrations of N, P, K and Mg; and a negative correlation with LDMC (Table 3). Thus, PC1 can be interpreted as the *leaf economy spectrum*. The second PC (PC2, 19% of total variation) had a positive correlation with Ni concentration and a negative correlation with carbon isotope discrimination (Δ) (Table 3). Given that Δ is used as a proxy of water use efficiency in C3 plants, we interpreted that the PC2 represents *hyperaccumulation and water use efficiency*. The third principal component (PC3, 16% of variance) had a positive correlation with Ca and a negative correlation with Mg concentrations (Table 3). It can be interpreted as the *equilibrium in Ca:Mg ratio*, a highly important parameter in ultramafic areas.

Table 3: PCA analysis of leaf traits. Variation explained by three principal components (PC1 to PC3) and loadings of leaf traits on those PCs. PCA was computed on a correlation matrix of log-transformed variables. Traits with high correlation with PCs (i.e. loadings > 0.5 or loadings < - 0.5) are marked in **bold** type.

	PC1	**PC2**	**PC3**
Variation explained (%)	41	19	16
Eigenvalue	3.73	1.75	1.41
Variable (trait) Loadings			
Specific Leaf Area (SLA)	**0.78**	- 0.49	- 0.03
Leaf Dry Matter Content (LDMC)	**- 0.85**	0.21	- 0.05
Leaf Carbon Isotope Discrimination (Δ)	0.27	**- 0.60**	0.48
Leaf Calcium concentration (Ca)	0.09	- 0.07	**0.84**
Leaf Potassium concentration (K)	**0.69**	0.48	0.33
Leaf Magnesium concentration (Mg)	**0.51**	- 0.40	**- 0.56**
Leaf Nitrogen concentration (N)	**0.90**	0.21	- 0.02
Leaf Nickel concentration (Ni)	0.20	**0.74**	0.03
Leaf Phosphorus concentration (P)	**0.85**	0.33	- 0.19

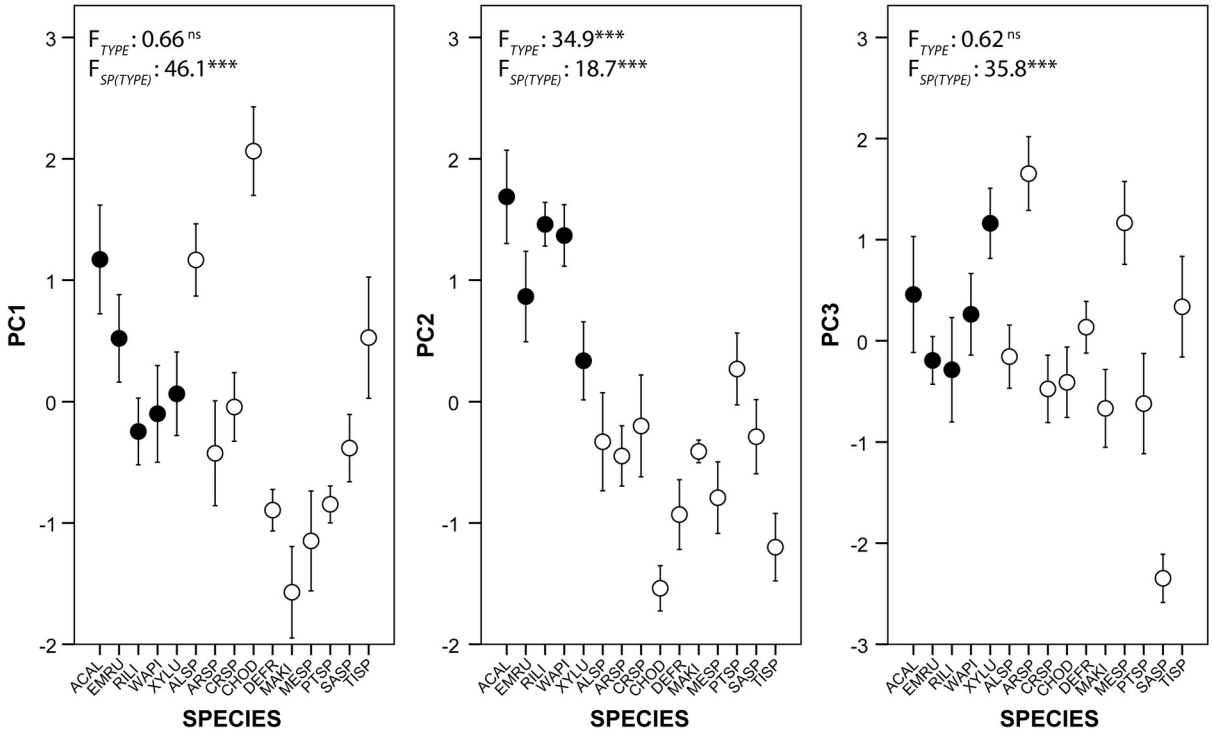

Figure 3: Species' scores on the three principal components (PCs) inferred by PCA analysis of nine leaf traits. Each dot indicates the average for each species and the whiskers mark the standard deviation (SD). Ni-hyperaccumulators are indicated by filled dots and non-hyperaccumulators by empty dots. The F's for the nested ANOVAs testing the effect of Type (F_{TYPE}) and of Species nested within Type ($F_{SP(TYPE)}$) are indicated. Species are arranged by type and then alphabetically. For species codes see table 1.

The results of nested ANOVAs indicated that the scores in PC2 (hyperaccumulation and water use efficiency) were different for hyperaccumulator and non-hyperaccumulator plants (hyperaccumulators had higher scores on PC2 than non-hyperaccumulators), whereas the scores in PC1 (leaf economics spectrum) and PC3 (Ca:Mg balance) were similar between groups of species (Fig. 3).

The linear mixed-effect models used to assess which traits influenced Ni accumulation in leaves showed congruent results with PC2, indicating that Ni foliar concentration was significantly affected by Δ ($P < 0.05$, Table S3). Adding clustering due to family or order to the model did not change or improve data fit within the models, indicating a non-significant impact of phylogenetic structure on trait relationships. A model selection analysis identified Δ and foliar K as the best traits combination to explain Ni foliar accumulation, performing similarly to the full model (all traits combined) but with less complexity (Table S3). However, none of the models could significantly explain Ni variance, suggesting that the binomial distribution of Ni leaf accumulation might be too

375 complex for one model. Therefore, Ni accumulation was modelled separately within
376 hyperaccumulator and non-hyperaccumulator species. The best model (selected) for
377 hyperaccumulator species indicates that leaf Ni significantly increases with Δ (Fig. 4a) and
378 decreases with K (Fig. 4b), accounting for 27% of the explained variance (Table S3). On the other
379 side, the best model (selected) for non-hyperaccumulator species indicates that leaf Ni significantly
380 increases with Mg (Fig. 4c) and decreases with K (Fig. 4b), accounting for 41% of the explained
381 variance (Table S3).

382

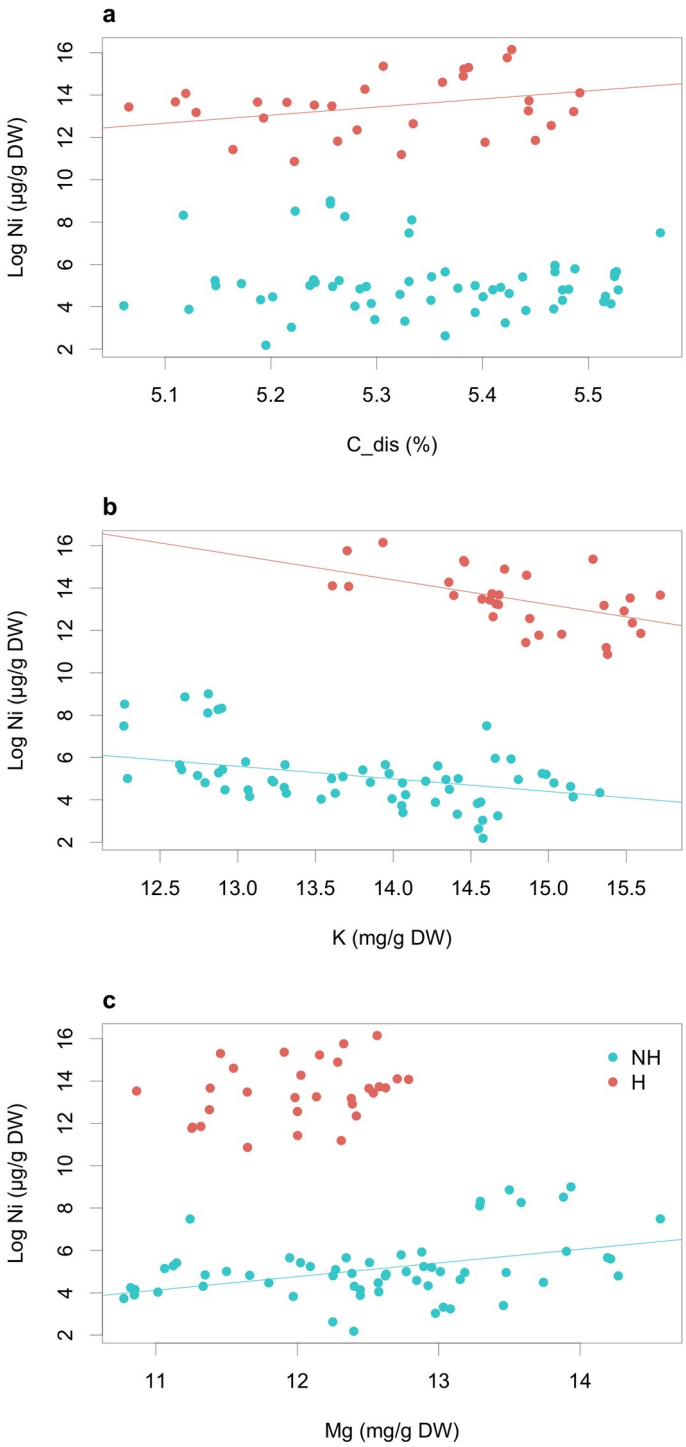

383

384 **Figure 4.** Biplots of the significant traits that modelled Ni accumulation for hyperaccumulator (H = red) and non-
385 hyperaccumulator (NH = blue) species groups, such as leaf carbon isotope discrimination (C_dis), leaf potassium
386 concentration (K) and leaf magnesium concentration (Mg). The line represents the variables that are significant (*P*
387 < 0.05) in Linear mixed models (LMMs) of each group. Please refer to table S3 for details on LMMs.

388

389

390

Discussion

In this study, we have explored the relationship between Ni hyperaccumulation and other traits involved in the leaf economics spectrum. Studies have shown that ultramafic vegetation has resource-conservative traits (Samojedny Jr et al. 2022) and we hypothesised that if hyperaccumulation were linked to efficient nutrient capture, hyperaccumulators would have a faster acquisitive strategy. Contrary to those hypotheses, hyperaccumulators did not show a distinct strategy on the leaf economics spectrum. Still, the leaf economics spectrum remains the main axis of variation within the ultramafic plant community (PC1 in Fig.3). Nickel hyperaccumulation was actually more correlated to the water-use efficiency spectrum inferred by carbon isotope discrimination (Δ) (PC2 in Fig.3). Lastly, a third axis of strategy variation reflects the capacity to regulate Ca and Mg in leaves (PC3 in Fig.3). Those three axes align well with the general constraints for plant growth on ultramafic soil, apart from metal excess: (1) nutrient acquisition, (2) water availability, and (3) Ca: Mg ratio (Kazakou et al. 2010; Palm and Van Volkenburgh 2014). Here, we suggest that those axes reflect the main environmental constraints that shape the resource acquisition strategies of the studied ultramafic plant community.

Leaf economics spectrum axis

According to the leaf economics spectrum expectations, plant species growing in restrictive environments such as ultramafic soils should adopt a slow strategy (i.e. low SLA, high LDMC, low nutrient concentrations, *etc*.) (Kazakou et al. 2008; Maestri et al. 2010; Reich 2014), as shown in studies of ultramafic plants in Greece (Adamidis et al. 2014), Italy (Lazzaro et al. 2021), Malaysia (Quintela-Sabarís et al. 2020), Spain (Hidalgo-Triana et al. 2023), and in a comparison of ultramafic and non-ultramafic communities from five regions across the world (Samojedny Jr et al. 2022). This tendency is also observed between ecotypes exposed to metalliferous and non-metalliferous soils (Wierzbicka and Pielichowska 2004), although some exceptions exist (e.g. Delhaye et al. 2016; Lange et al. 2017b). Here, we observed a similar tendency in community-level traits, as the average specific leaf area and LDMC were found on the more conservative side of the leaf economics spectrum compared to the worldwide average (Table 2) (Kattge et al. 2011). However, despite the scarcity of nutrients in the soil, the average nutrient foliar concentrations of hyperaccumulators were above the global average values reported for plants (Kattge et al. 2011) or for evergreen angiosperms (Vergutz et al. 2012), highlighting the complexity of interpreting leaf economics spectrum strategies in metallophyte communities.

Indeed, the leaf economics spectrum appears clearly as the main variation factor within our ultramafic plant community (PC1 = 41%, Fig.4), which is in accordance with the observation that other plant communities from metal-rich soils maintain a substantial functional diversity (Delhaye

et al. 2020, 2024). Moreover, our results showed that Ni contributed to PC2 which is orthogonal (i.e. not-correlated) to PC1(leaf economics spectrum axis), suggesting that other factors different from Ni accumulation are primarily linked to leaf economics spectrum strategies development (Reich 2014). Our results also showed the decoupling of the leaf economics spectrum from the water (PC2) and Ca: Mg acquisition axes (PC3), pointing to macronutrients and soil fertility as the potential factors primarily affecting the leaf economics spectrum in this ultramafic plant community. Similarly, several studies of metallophyte communities of Cu-Co hills showed that soil fertility was the major factor affecting specific leaf area and LDMC of metallophytes, rather than the plant Cu or Co accumulation (Delhaye et al. 2016, 2019, 2020; Lange et al. 2017b). Moreover, other phenomena not considered in our study, such as interspecific competition or facilitation (i.e. creating microenvironments from positive plant-soil feedback of pioneer species) may favour divergent strategies in the leaf economics spectrum (Delhaye et al. 2024), making more complicated to identify global patterns of variation in metal-rich environments.

Hyperaccumulation and Water-use efficiency axis

The nANOVA analyses indicated that hyperaccumulators had significantly higher scores than non-hyperaccumulators in PC2. This PC is a composite factor that opposed Ni accumulation to carbon isotope discrimination (Δ), a trait related to water-use efficiency (e.g. Farquhar et al. 1989). Conversely, LMMs suggested a positive relationship between leaf Ni and Δ (Table S3). This contradiction could be explained by the distinct strategies exhibited between hyperaccumulator and non-hyperaccumulator species on this water-use efficiency spectrum. Indeed, only hyperaccumulator species harbour a significant and positive relationship between leaf Ni accumulation and Δ ($P < 0.05$). This relationship suggests that, in hyperaccumulators, the higher the Ni accumulation, the higher the stomatal conductance, which implies higher transpiration and lower water-use efficiency. Our result is congruent with those obtained by Scartazza et al. (2022), who found that high Ni doses had a stimulatory effect on stomatal opening and transpiration fluxes in the strong Ni hyperaccumulator *Odontarrhena chalcidica*, but not in the weak and medium hyperaccumulators *O. muralis* and *O. moravensis*. Moreover, Ni concentration in hyperaccumulator species was significantly and negatively modelled by K foliar accumulation, which is also a trait linked to plant water economy by its direct role in stomatal opening, plant cell turgor, water uptake and water transportation from roots to shoots (Hasanuzzaman et al. 2018; Johnson et al. 2022). This result suggests an antagonistic relationship between K and Ni accumulation, where Ni might partially replace K in its role in plant water balance.

The fact that Δ and K, two factors linked to plant water economy, were the best explanatory variables of Ni hyperaccumulation ($R^2 = 0.27$), suggests that Ni hyperaccumulation is linked to

water-use efficiency capacities. The role of Ni in osmoregulation and water-use efficiency was proposed by Baker and Walker (1990), confirmed in the Australian Ni hyperaccumulator *Stackhousia tryonii* (Bhatia et al. 2005), and recent studies support a role of hyperaccumulation in the tolerance to drought stress: the abovementioned work by Scartazza et al. (2022), and the work by Delhaye et al. (2024), who found original functional trait combinations in the Ni hyperaccumulator *Odontarrhena lesbiaca* which the authors interpreted as possibly being linked to a higher tolerance to drought. In contrast, Wan et al. (2015) found that increased transpiration was the main driver of arsenic (As) hyperaccumulation and redistribution in the fern *Pteris vittata*. Future studies will be needed to assess whether Ni hyperaccumulation is the driver of transpiration or the result of enhanced transpiration.

Ca:Mg ratio axis

A low soil Ca: Mg ratio is one of the main constraints for plant growth on ultramafic soil (Palm and Van Volkenburgh 2014). Although the present soil has a ratio of exchangeable Ca: Mg (1.71) higher than usual in ultramafic soils (0.2 – 0.9; Kierczak et al. 2007), the total amount of Mg remains consistently higher than Ca (Ca: Mg = 0.26). This poses a risk of Ca deficiency for plants, as soil Mg can have antagonistic effects on Ca absorption. To avoid this limitation, many ultramafic plants developed unique adaptations to limit Mg absorption, translocation, or accumulation (Palm and Van Volkenburgh 2014), or to increase their Mg metabolic needs (Brady et al. 2005), and higher Ca:Mg ratios have been observed in ultramafic species compared to congeneric non-ultramafic taxa (O'Dell et al. 2006; Quintela-Sabarís et al. 2017). Therefore, it is not surprising to find that the third axis of variation (PC3) in our community is based on Ca and Mg in leaves. It reflects the ability to manage a low Ca: Mg ratio, more precisely, to manage Mg excess in soil. The accumulation of Mg is a significant component of the PCA (PC1 and PC3), where it correlates positively to specific leaf area and N, P, K concentrations, and negatively to Ca (antagonist). It suggests that Mg management might be a key component in the resource acquisition and metal accumulation strategies of ultramafic plants.

Hyperaccumulators tend to accumulate less Mg (2.4 mg g^{-1}) than other non-hyperaccumulator species (4.1 mg/g), suggesting that they seem able to restrict Mg absorption, translocation, and/or accumulation in their leaves, in opposition to their Ni hyperaccumulation ability. This adaptation allows them to have a Ca:Mg ratio in leaves almost twice as large as non-hyperaccumulators (Ca: Mg respectively of 6.2 and 3.7). The present study does not allow an understanding of the underlying mechanisms to explain this tendency, but a trade-off might exist between Mg and Ni accumulation. Some studies support that increasing Ca:Mg in leaves provides better protection

against metal toxicity (Brady, 2005). Mg excess was also suggested as an antagonist to K and N, thereby, playing a role in other macronutrient acquisitions (Proctor and Woodell 1975). Conversely, leaf Mg concentrations increase significantly with Ni in non-hyperaccumulator species (Table S3), highlighting the different Mg uptake strategies between the two groups. A similar correlation between Ni and Mg was found in plants from ultramafic soils from northern Morocco (Ater et al. 2000). Although this correlation does not provide explanations, it suggests that non-hyperaccumulator species had similar mechanisms to cope with excess of Ni and Mg, as both elements seem to be either excluded or moderately accumulated simultaneously.

Indirect linkage between Ni hyperaccumulation and nutrient acquisition

Even if hyperaccumulator species did not possess a significantly different strategy on the leaf economics spectrum, they tend to have higher leaf concentrations of N, P, and K compared to non-hyperaccumulators (Table 2), implying greater nutrient acquisition capacities. In a recent experiment comparing the concentrations of several elements in plants growing in nickel-spiked soils, Meindl et al. (2021) found that Ni hyperaccumulators had higher foliar concentrations of K compared to non-hyperaccumulators. Scartazza et al. (2022) also found a positive relationship between Ni concentration and N allocated to leaf photosynthetic components in hyperaccumulators. The authors interpreted these observations as a support of the inadvertent uptake hypothesis (i.e. hyperaccumulation is the result of efficient nutrient-scavenging mechanisms in nutrient-poor soils). Our results point in a similar direction, suggesting an indirect (and so less significant) link between Ni hyperaccumulation and nutrient acquisition. Considering the possible relationship between hyperaccumulation and water-use efficiency obtained in this study, we can speculate that increased transpiration might be the mechanism responsible for higher nutrient uptake tendencies.

Conclusions

This study reveals that Ni hyperaccumulation on Sabah ultramafic soils is not linked to the leaf economics spectrum as a whole but rather to water use efficiency strategies due to correlation with carbon isotope discrimination and K, suggesting that water scarcity is the main environmental constraint that induced hyperaccumulation behaviour. These results support some hypotheses about the role of Ni hyperaccumulation in drought resistance and osmoregulation (Baker and Walker 1990; Bhatia et al. 2005). However, other studies also have found different traits correlated to ultramafic tolerance and hyperaccumulation, notably on the leaf economic spectrum (Adamidis et al. 2014; Delhaye et al. 2024; Lazzaro et al. 2021). This aligned with the many conclusions that hyperaccumulation arose separately many times in the evolutionary tree of plants, rooted in strong environmental pressure (Baker et al. 2010) and resulting in different functional strategies (Gervais-

Bergeron et al. 2023). Here, traits were proved to be valuable tools to understand the strategies of hyperaccumulators and to distinguish the environmental factors that might have induced this unique behaviour. Further experiments are needed to obtain in-depth knowledge on the mechanisms involved in the relationship between hyperaccumulation, environmental constraints, and functional traits.

Acknowledgements

Sabah Biodiversity Centre provided C. Quintela-Sabarís with the Access and Export Licences to develop this research in Sabah (Malaysia). Local support provided by Mr. Sahlan Sukaibin and personnel in Monggis Substation (Kinabalu Park) is warmly acknowledged. C. Quintela-Sabarís Postdoctoral contract and this research have been funded by the French National Research Agency through the national program "Investissements d'avenir" with the reference ANR-10-LABX-21-01/LABEX RESSOURCES21, and by Region Lorraine (France). The authors also acknowledge Miguel Gonzalez-Szamocki for assistance with language editing. Funding for open access charge: Universidade de Vigo/CISUG.

References

Adamidis GC, Kazakou E, Aloupi M, Dimitrakopoulos PG (2016) Is it worth hyperaccumulating Ni on non-serpentine soils? Decomposition dynamics of mixed-species litters containing hyperaccumulated Ni across serpentine and non-serpentine environments. Ann Bot 117:1241–1248

Adamidis GC, Kazakou E, Fyllas NM, Dimitrakopoulos PG (2014) Species adaptive strategies and leaf economic relationships across serpentine and non-Serpentine habitats on Lesbos, Eastern Mediterranean. PLoS ONE. https://doi.org/10.1371/journal.pone.0096034

AFNOR (1995) NF ISO 11263. Soil quality. Determination of phosphorus. Spectrometric determination of phosphorus in sodium hydrogen carbonate solution. Current standard.

AFNOR (1999) NF X31-130. Soil quality. Chemical methods. Determination of cationic exchange capacity (CEC) and extractible cations. Current standard.

Aiba S, Kitayama K (1999) Structure, composition and species diversity in an altitude-substrate matrix of rain forest tree communities on Mount Kinabalu, Borneo. Plant Ecol 140:139–157

Ater M, Lefèbvre C, Gruber W, Meerts P (2000) A phytogeochemical survey of the flora of ultramafic and adjacent normal soils in North Morocco. Plant Soil 218:127–135

Baker AJM, McGrath SP, Reeves RD, Smith JAC (2000) Metal hyperaccumulator plants: a review of the ecology and physiology of a biological resource for phytoremediation of metal-polluted soils. In: Terry N, Bañuelos G (eds) Phytoremediation of Contaminated Soil and Water. CRC Press, Boca Raton, pp 85–107

Baker AJM, Walker PL (1990) Ecophysiology of metal uptake by tolerant plants. In: Shaw AJ (ed) Heavy Metal Tolerance in Plants: Evolutionary Aspects. CRC Press, Boca Raton, pp 155–177

569 Baker AJM, Ernst WHO, van der Ent A, Malaisse F, Ginocchio R (2010) Metallophytes: The
570 unique biological resource, its ecology and conservational status in Europe, central Africa
571 and Latin America. In: Hallberg KB, Batty LC (eds) Ecology of industrial pollution.
572 Cambridge University Press, Cambridge, pp 7–40.
573 https://doi.org/10.1017/CBO9780511805561.003

574 Bhatia NP, Baker AJM, Walsh KB, Midmore DJ (2005) A role for nickel in osmotic adjustment in
575 drought-stressed plants of the nickel hyperaccumulator Stackhousia tryonii Bailey. Planta
576 223:134–139

577 Boyd RS (2007) The defense hypothesis of elemental hyperaccumulation: status, challenges and
578 new directions. Plant Soil 293:153–176. https://doi.org/10.1007/s11104-007-9240-6

579 Boyd RS (2004) Ecology of metal hyperaccumulation. New Phytol 162:563–567.
580 https://doi.org/10.1111/j.1469-8137.2004.01079.x

581 Brady KU, Kruckeberg AR, Bradshaw HD (2005) Evolutionary Ecology of Plant Adaptation to
582 Serpentine Soils. Annu Rev Ecol Evol Syst 36:243–266.
583 https://doi.org/10.1146/annurev.ecolsys.35.021103.105730

584 Brooks RR (1987) Serpentine and its vegetation: a multidisciplinary approach. Dioscorides Press,
585 Portland

586 Bruand A, Duval O, Gaillard H, Darthout R, Jamagne M (1996) Variabilité des propriétés de
587 rétention en eau des sols: importance de la densité apparente. Etud Gest Sols 31:27–40

588 Cornelissen JHC, Lavorel S, Garnier E, Diaz S, Buchmann N, Gurvich DE, Reich PB, ter Steege H,
589 Morgan HD, van der Heijden MGA, Pausas JG, Poorter H (2003) A handbook of protocols
590 for standardised and easy measurements of plant functional traits worldwide. Aust J Bot
591 51:335–380

592 Delhaye G, Bauman D, Séleck M, Ilunga wa Ilunga E, Mahy G, Meerts P (2020) Interspecific trait
593 integration increases with environmental harshness: A case study along a metal toxicity
594 gradient. Funct Ecol 34:1428–1437. https://doi.org/10.1111/1365-2435.13570

595 Delhaye G, Dimitrakopoulos PG, Adamidis GC (2024) Interspecific trait differences drive plant
596 community responses on serpentine soils. J Ecol 112:2887–2900.
597 https://doi.org/10.1111/1365-2745.14429

598 Delhaye G, Hardy OJ, Séleck M, Ilunga wa Ilunga E, Mahy G, Meerts P, Kühn I (2020) Plant
599 community assembly along a natural metal gradient in central Africa: Functional and
600 phylogenetic approach. J Veg Sci 31:151–161. https://doi.org/10.1111/jvs.12829

601 Delhaye G, Violle C, Séleck M, Ilunga wa Ilunga E, Daubie I, Mahy G, Meerts P, Goslee S (2016)
602 Community variation in plant traits along copper and cobalt gradients. J Veg Sci 27:854–
603 864. https://doi.org/10.1111/jvs.12394

604 Diaz S, Kattge J, Cornelissen JHC, Wright IJ, Lavorel S, Dray S, Reu B, Kleyer M, Wirth C,
605 Prentice IC, Garnier E, Bonisch G, Westoby M, Poorter H, Reich PB, Moles AT, Dickie J,
606 Gillison AN, Zanne AE, Chave J, Wright SJ, Sheremet'ev SN, Jactel H, Baraloto C,
607 Cerabolini B, Pierce S, Shipley B, Kirkup D, Casanoves F, Joswig JS, Gunther A, Falczuk
608 V, Ruger N, Mahecha MD, Gorne LD (2016) The global spectrum of plant form and
609 function. Nature 529:167–171

610 El Mehdawi AF, Pilon-Smits EAH (2012) Ecological aspects of plant selenium hyperaccumulation.
611 Plant Biol 14:1–10

612 Farquhar GD, Ehleringer JR, Hubick KT (1989) Carbon Isotope Discrimination and Photosynthesis.
613 Annu Rev Plant Physiol Plant Mol Biol 40:503–537.
614 https://doi.org/10.1146/annurev.pp.40.060189.002443

615 Fones HN, Eyles CJ, Bennett MH, Smith JAC, Preston GM (2013) Uncoupling of reactive oxygen
616 species accumulation and defence signalling in the metal hyperaccumulator plant Noccaea
617 caerulescens. New Phytol 199:916–924

618 Garcia de la Torre VS, Majorel-Loulergue C, Gonzalez DA, Soubigou-Taconnat L, Rigaill GJ,
619 Pillon Y, Barreau L, Thomine S, Fogliani B, Burtet-Sarramegna V, Merlot S (2018) Wide
620 cross-species RNA-Seq comparison reveals convergent molecular mechanisms involved in
621 nickel hyperaccumulation across dicotyledons. New Phytol 229:994–1006

622 Garnier E, Cortez J, Billès G, Navas ML, Roumet C, Debussche M, Laurent G, Blanchard A, Aubry
623 D, Bellmann A (2004) Plant functional markers capture ecosystem properties during
624 secondary succession. Ecology 85:2630–2637

625 Garnier E, Navas ML (2013) Diversité fonctionnelle des plantes: traits des organismes, structure
626 des communautés, propriétés des écosystèmes: cours. De Boeck, Brussels.

627 Hasanuzzaman M, Bhuyan MHMB, Nahar K, Hossain MS, Al Mahmud J, Hossen MS, Masud
628 AAC, Moumita, Fujita M (2018) Potassium: A vital regulator of plant responses and
629 tolerance to abiotic stresses. Agronomy 8:31. https://doi.org/10.3390/agronomy8030031

630 Hidalgo-Triana N, Pérez-Latorre AV, Adomou AC, Rudner M, Thorne JH (2023) Adaptations to
631 the stressful combination of serpentine soils and Mediterranean climate drive plant
632 functional groups and trait richness. Front Plant Sci 14:1040839.
633 https://doi.org/10.3389/fpls.2023.1040839

634 Jaffré T, Pillon Y, Thomine S, Merlot S (2013) The metal hyperaccumulators from New Caledonia
635 can broaden our understanding of nickel accumulation in plants. Front Plant Sci 4:279.
636 https://doi.org/10.3389/fpls.2013.00279

637 Jin Y, Qian H (2019) V.Phylomaker: an R package that can generate very large phylogenies for
638 vascular plants. Ecography 42:1353–1359

639 Johnson R, Vishwakarma K, Hossen MS, Kumar V, Shackira AM, Puthur JT, Abdi G, Sarraf M,
640 Hasanuzzaman M (2022) Potassium in plants: Growth regulation, signaling, and
641 environmental stress tolerance. Plant Physiol Biochem 172:56-69.
642 https://doi.org/10.1016/j.plaphy.2022.01.001

643 Kazakou E, Adamidis GC, Baker AJM, Reeves RD, Godino M, Dimitrakopoulos PG (2010)
644 Species adaptation in serpentine soils in Lesbos Island (Greece): Metal hyperaccumulation
645 and tolerance. Plant Soil 332:369–385. https://doi.org/10.1007/s11104-010-0302-9

646 Kazakou E, Dimitrakopoulos PG, Baker AJM, Reeves RD, Troumbis AY (2008) Hypotheses,
647 mechanisms and trade-offs of tolerance and adaptation to serpentine soils: from species to
648 ecosystem level. Biol Rev 83:495–508

649 Kierczak J, Neel C, Bril H, Puziewicz J (2007) Effect of mineralogy and pedoclimatic variations on
650 Ni and Cr distribution in serpentine soils under temperate climate. Geoderma 142:165–177

651 Kitayama K, Aiba SI, Majalap-Lee N, Ohsawa M (1998) Soil nitrogen mineralization rates of
652 rainforests in a matrix of elevations and geological substrates on Mount Kinabalu, Borneo.
653 Ecol Res 13:301–312

654 Krämer U (2010) Metal hyperaccumulation in plants. Ann Revi Plant Biol 61:517–534

655 Kuznetsova A, Brockhoff PB, Christensen RHB, Jensen SP (2020). lmerTest: Tests in Linear
656 Mixed Effects Models, v 3.1-3. https://cran.r-project.org/web/packages/lmerTest/index.html

657 Lambers H, Chapin FS, Pons TL (2008) Plant physiological ecology, 2nd edn. Springer, New York.

658 Lambers H, Hayes PE, Laliberté E, Oliveira RS, Turner BL (2015) Leaf manganese accumulation
659 and phosphorus-acquisition efficiency. Trends Plant Sci 20:83–90

Lange B, van der Ent A, Baker AJM, Echevarria G, Mahy G, Malaisse F, Meerts P, Pourret O, Verbruggen N, Faucon MP (2017a) Copper and cobalt accumulation in plants: a critical assessment of the current state of knowledge. New Phytol 213:537–551

Lange B, Faucon MP, Delhaye G, Hamiti N, Meerts, P (2017b) Functional traits of a facultative metallophyte from tropical Africa: Population variation and plasticity in response to cobalt. Environ Exp Bot 136:1–8. https://doi.org/10.1016/j.envexpbot.2016.12.010

Lazzaro L, Colzi I, Ciampi D, Gonnelli C, Lastrucci L., Bazihizina N, Viciani D, Coppi A (2021) Intraspecific trait variability and genetic diversity in the adaptive strategies of serpentine and non-serpentine populations of Silene paradoxa L. Plant Soil 460:105–121. https://doi.org/10.1007/s11104-020-04780-1

Lindsay WL, Norvell WA (1978) Development of a DTPA soil test for zinc, iron, manganese, and copper. Soil Sci Soc Am J 42:421–428.

Maestri E, Marmiroli M, Visioli G, Marmiroli N (2010) Metal tolerance and hyperaccumulation: Costs and trade-offs between traits and environment. Environ Exp Bot 68:1–13. https://doi.org/10.1016/j.envexpbot.2009.10.011

Mazerolle MJ (2020) AICcmodavg: Model selection and multimodel inference based on (Q)AIC(c). Version 2.3-1. https://CRAN.R-project.org/package=AICcmodavg

Meindl GA, Poggioli MI, Bain DJ, Colón MA, Ashman TL (2021) A test of the inadvertent uptake hypothesis using plang species adapted to serpentine soil. Soil Syst 5:34. https://doi.org/10.3390/soilsystems5020034

Merlot S, García de la Torre VS, Hanikenne M (2018) Physiology and molecular biology of trace element hyperaccumulation. In: van der Ent A, Echevarria G, Baker AJM, Morel JL (eds) Agromining: Farming for Metals. Springer, Cham, pp 93–116.

O'Dell R, James JJ, Richards JH (2006) Congeneric serpentine and nonserpentine shrubs differ more in leaf Ca:Mg than in tolerance to low N, low P, or heavy metals. Plant Soil 280:49–64.

Pollard AJ, Reeves RD, Baker AJM (2014) Facultative hyperaccumulation of heavy metals and metalloids. Plant Sci 217:8–17.

Posit team (2023) RStudio: integrated development environment for R. Posit Sofware, PBC, Boston, MA. https://www.posit.co/.

Proctor J, Lee YF, Langley AM, Munro WRC, Nelson T (1988) Ecological studies on Gunung Silam, a small ultrabasic mountain in Sabah, Malaysia. I. Environment, forest structure and floristics. J Ecol 76:320–340.

Proctor J, Woodell SRJ (1975) The Ecology of Serpentine Soils. In: MacFadyen A (ed) Advances in Ecological Research, Vol. 9. Academic Press, London, pp 255–366 https://doi.org/10.1016/S0065-2504(08)60291-3

Qian H, Jin Y (2016) An update megaphylogeny of plants, a tool for generating plant phylogenies and an analysis of phylogenetic community structure. J Plant Ecol 9:233–239.

Quintela-Sabarís C, Marchand L, Smith JAC, Kidd PS (2017) Using AFLP genome scanning to explore serpentine adaptation and nickel hyperaccumulation in Alyssum serpyllifolium. Plant Soil 416:391–408.

Quintela-Sabarís C, Faucon MP, Repin R, Sugau JB, Nilus R, Echevarria G, Leguédois S (2020) Plant functional traits on tropical ultramafic habitats affected by fire and mining: insights for reclamation. Diversity 12:248. https://doi.org/10.3390/d12060248

R Core Team (2022) R: A language and environment for statistical computing. https://www.R-project.org/.

706 Rascio N, Navari-Izzo F (2011) Heavy metal hyperaccumulating plants: how and why do they do
707 it? And what makes them so interesting? Plant Sci 180:169–181.

708 Reeves RD, Baker AJM, Jaffré T, Erskine PD, Echevarria G, van der Ent A (2018) A global
709 database for plants that hyperaccumulate metal and metalloid trace elements. New Phytol
710 218:407–411.

711 Reich PB (2014) The world-wide 'fast–slow' plant economics spectrum: a traits manifesto. J Ecol
712 102:275–301. https://doi.org/10.1111/1365-2745.12211

713 Revell LJ (2012) phytools: an R package for phylogenetic comparative biology (and other things).
714 Methods Ecol Evol 3:217–223.

715 Samojedny Jr TJ, Garnica-Díaz C, Grossenbacher DL, Adamidis GC, Dimitrakopoulos PG, Siebert
716 SJ, Spasojevic MJ, Hulshof CM, Rajakaruna N (2022) Specific leaf area is lower on
717 ultramafic than on neighbouring non-ultramafic soils. Plant Ecol Diversity 15:243–252.

718 Scartazza A, Di Baccio D, Mariotti L, Bettarini I, Selvi F, Pazzagli L, Colzi I, Gonnelli C (2022)
719 Photosynthesizing while hyperaccumulating nickel: Insights from the genus Odontarrhena
720 (Brassicaceae). Plant Physiol Biochem 176:9–20.

721 Schneider CA, Rasband WS, Eliceiri KW (2012) NIH Image to ImageJ: 25 years of image analysis.
722 Nature Methods 9:671.

723 van der Ent A, Baker AJM, Reeves RD, Pollard AJ, Schat H (2013) Hyperaccumulators of metal
724 and metalloid trace elements: facts and fiction. Plant Soil 362:319–334.

725 van der Ent A, Cardace D, Tibbett M, Echevarria G (2017) Ecological implications of pedogenesis
726 and geochemistry of ultramafic soils in Kinabalu Park (Malaysia). Catena 160: 154–169.
727 https://doi.org/10.1016/j.catena.2017.08.015

728 van der Ent A, Echevarria G, Tibbett M (2016) Delimiting soil chemistry thresholds for nickel
729 hyperaccumulator plants in Sabah (Malaysia). Chemoecology 26:1–16.

730 van der Ent A, Erskine PD, Sumail S (2015a) Ecology of nickel hyperaccumulator plants from
731 ultramafic soils in Sabah (Malaysia). Chemoecology 25:243–259.

732 van der Ent A, Ocenar A, Tisserand R, Sugau JB, Echevarria G, Erskine PD (2019) Herbarium X-
733 ray fluorescence screening for nickel, cobalt and manganese hyperaccumulator plants in the
734 flora of Sabah (Malaysia, Borneo Island). J Geochem Explo 202:49–58.

735 van der Ent A, van Balgooy M, van Welzen PC (2015b) Actephila alanbakeri (Phyllanthaceae): a
736 new nickel hyperaccumulating plant species from localised ultramafic outcrops in Sabah
737 (Malaysia). Bot Stud 57:6.

738 Van Gils H, Delfino J, Rugege D, Janssen L (2004) Efficacy of Chromolaena odorata control in a
739 South African conservation forest. S Afr J Sci 100:251–253.

740 Wan XM, Lei M, Chen TB, Yang JX, Liu HT, Chen Y (2015) Role of transpiration in arsenic
741 accumulation of hyperaccumulator Pteris vittata L. Environ Sci Pollut Res 22:16631–16639.

742 Wierzbicka M, Pielichowska M (2004 Adaptation of *Biscutella laevigata* L, a metal
743 hyperaccumulator, to growth on a zinc-lead waste heap in southern Poland. I: Differences
744 between waste-heap and mountain populations. Chemosphere 54:1663–1674.
745 https://doi.org/10.1016/j.chemosphere.2003.08.031

746 Wilson PJ, Thompson K, Hodgson JG (1999) Specific leaf area and leaf dry matter content as
747 alternative predictors of plant strategies. New Phytol 143:155–162.
748 https://doi.org/10.1046/j.1469-8137.1999.00427.x

749 Wright IJ, Reich PB, Westoby M, Ackerly DD, Baruch Z, Bongers F, Cavender-Bares J, Chapin T,
750 Cornelissen JHC, Diemer M, Flexas J, Garnier E, Groom PK, Gulias J, Hikosaka K, Lamont

BB, Lee T, Lee W, Lusk C, Midgley JJ, Navas ML, Niinemets Ü, Oleksyn J, Osada N, Poorter H, Poot P, Prior L, Pyankov VI, Roumet C, Thomas SC, Tjoelker MG, Veneklaas EJ, Villar R (2004) The worldwide leaf economics spectrum. Nature 428:821–827. https://doi.org/10.1038/nature02403

Statements and Declarations

Funding

Open Access funding provided thanks to the CRUE-CSIC agreement with Springer Nature. C. Quintela-Sabarís Postdoctoral contract and this research have been funded by the French National Research Agency through the national program "Investissements d'avenir" with the reference ANR-10-LABX-21-01/LABEX RESSOURCES21, and by Region Lorraine (France).

Competing interests

The authors have no relevant financial or non-financial interests to disclose.

Author Contributions

All authors contributed to the study conception and design. Field campaign preparation and sampling were performed by C Quintela-Sabarís, Sukaibin Sumail, Rimi Repin, John Sugau and Reuben Nilus. Data collection and analysis were performed by C Quintela-Sabarís, M-P Faucon and B Gervais-Bergeron. The first draft of the manuscript was written by C Quintela-Sabarís, and B Gervais-Bergeron, and all authors commented on previous versions of the manuscript. All authors read and approved the final manuscript.

Data availability

The dataset supporting this publication is available online, under a Creative Commons Attribution 4.0 International (CC-BY-4.0), at the Zenodo repository: https://doi.org/10.5281/zenodo.14587651